Electronic Supplementary Material (ESI) for Inorganic Chemistry Frontiers.
This journal is © the Partner Organisations 2022

Supporting Information

The critical role of ligand topology: strikingly different properties of Gd(III) complexes with regioisomeric AAZTA derivatives

Jonathan Martinelli,[a] Mariangela Boccalon,[b] David Horvath,[b] David Esteban-Gomez,[c] Carlos Platas Iglesias,[c] Zsolt Baranyai[b*] and Lorenzo Tei.[a*]

---

[a] *Dipartimento di Scienze e Innovazione Tecnologica, Università del Piemonte Orientale "A. Avogadro", Viale T. Michel 11, 15121 Alessandria, Italy*

[b] *Bracco Research Centre, Bracco Imaging S.p.A. Via Ribes 5, 10010, Colleretto Giacosa, Italy.*

[c] *Universidade da Coruña, Centro de Investigacións Científicas Avanzadas (CICA) and Departamento de Química Fundamental, Facultade de Ciencias, 15071, A Coruña, Galicia, Spain.*

Table of contents

1. Thermodynamic and kinetic studies of the Gd(III)-complexes

1.1. Protonation and complexation properties of AAZ3A-endoHB and AAZ3A-exoHB

The protonation sequence and the protonation constants of AAZ3A-endoHB ligands, defined by Equation S1, were determined by recording the absorption spectra of the ligand in the pH range 2.0-11.5. Absorption spectra of AAZ3A-endoHB as a function of pH are shown in Figure S1.

$$K_i^H = \frac{[H_iL]}{[H_{i-1}L][H^+]} \qquad i=1, 2\ldots6. \qquad (S1)$$

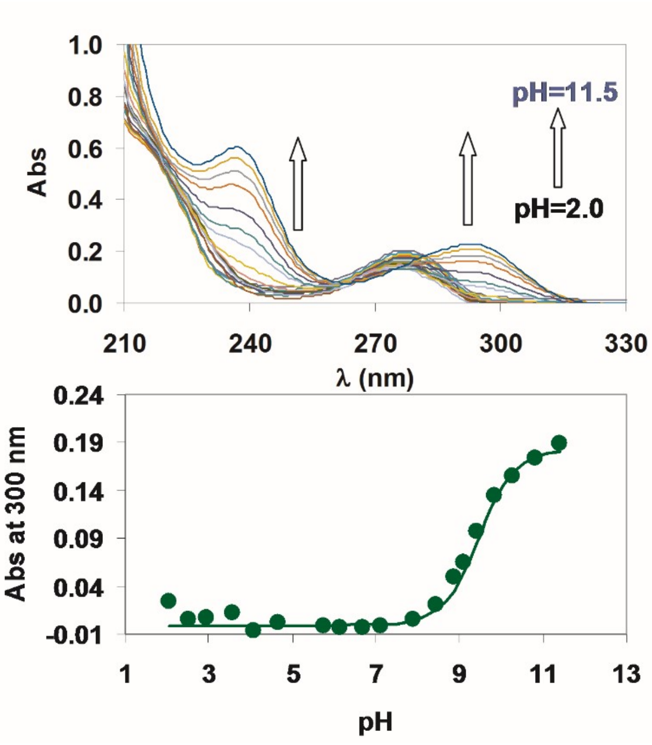

Figure S1. Absorption spectra of AAZ3A-endoHB and the measured absorbance values at 300 nm ([AAZ3A-endoHB]=60 µM, 0.15 M NaCl, 25 °C).

The absorbance values at each wavelength can be expressed by the sum of the absorption of each species:[1]

$$A = \sum c_i l \varepsilon_i \qquad (S2)$$

where i = 0, 1, 2,…,n and c_i, l and ε_i are the concentration, the path length and the molar absorptivity of the involved species, respectively. By taking into account of the total concentration ($[L]_t=[L]+[HL]+[H_2L]+\ldots+[H_nL]$) and the protonation constants of the AAZ3A-endoHB ligand ($\alpha_H = 1+K_1[H^+]+K_1K_2[H^+]^2+\ldots+K_1K_2\ldots K_n[H^+]^n$), Equation S2 can be expressed in the following form (l can be neglected by using the same cuvette):

$$A = \frac{\varepsilon_L}{\alpha_H} + \frac{\varepsilon_{HL}K_1[H^+]}{\alpha_H} + \frac{\varepsilon_{H_2L}K_1K_2[H^+]^2}{\alpha_H} + \ldots + \frac{\varepsilon_{H_nL}K_1K_2 \ldots K_n[H^+]^n}{\alpha_H} \qquad (S3)$$

The protonation constants and the molar absorptivity of each protonated species formed by AAZ3A-endoHB were calculated by fitting the pH – absorbance data (Figure S1) to Equation S3. However, $\log K_\mathrm{i}^\mathrm{H}$=9.2(1) value could be evaluated only by fitting the pH-absorbance data with the reasonable error. According to the spectral changes, it can be assumed that the $\log K_\mathrm{i}^\mathrm{H}$=9.2(1) value characterizes the protonation of the phenol group in AAZ3A-endoHB ligand.

The stepwise protonation of AAZTA was investigated by following the ^{1}H-NMR chemical shifts of non-labile protons as a function of pH.[2] The first and second protonation processes take place at the exocyclic and ring nitrogen atoms, respectively. The first protonation occurs partially at the exocyclic and a ring N-atom, while the first proton is transferred to the exocyclic nitrogen in the second protonation process due to the electrostatic repulsion between the protonated ring and the exocyclic nitrogen. Further protonations occur at one of the ring-carboxylate groups, at the non-protonated ring nitrogen atom and/or at the carboxylate pendant arms, respectively. By considering the protonation constant of AAZ3A-endoHB obtained by spectrophotometry ($\log K_\mathrm{i}^\mathrm{H}$=9.2(1), 0.15 M NaCl, 25 °C) and the protonation constant of phenol ($\log K^\mathrm{H}$=10.0, 0.1 M $NaClO_4$, 25 °C)[3] it is reasonable to assume that the second protonation of AAZ3A-endoHB and AAZ3A-exoHB ligands involves the phenol group of the pendant arm.

1.1.2. Complexation properties of ligands

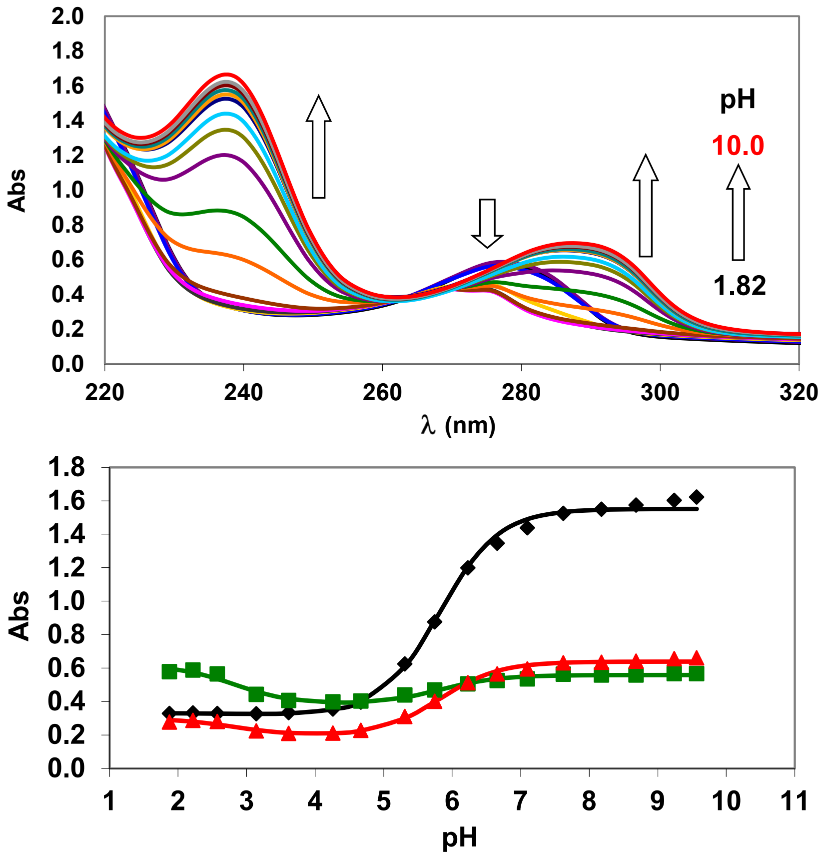

Figure S2. Absorption spectra and absorbance values of Gd^{3+} - AAZ3A-endoHB system at 238 (◷), 275 (O) and 291 nm (□) ($[Gd^{3+}]$=[AAZ3A-endoHB]=0.2 mM, 0.15 M NaCl, 25 °C)

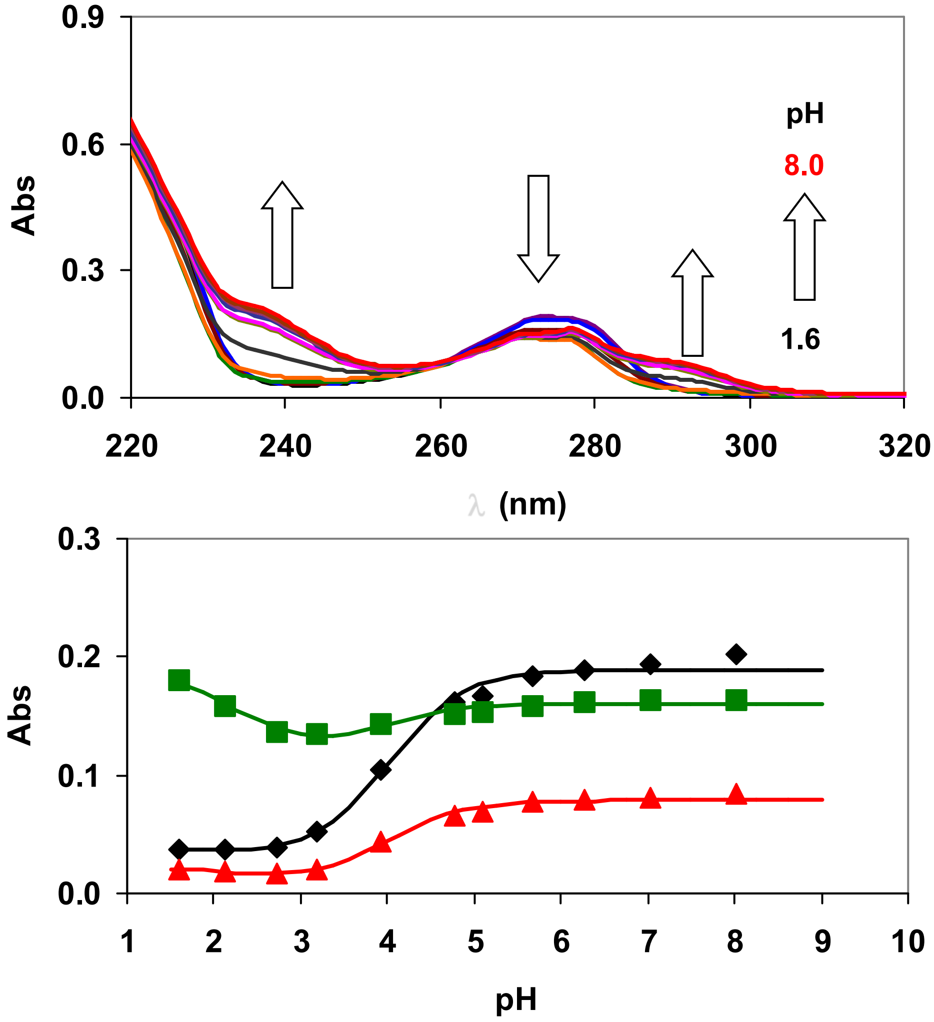

Figure S3. Absorption spectra and absorbance values of Gd^{3+} - AAZ3A-exoHB system at 238 (◷), 275 (O) and 291 nm (□

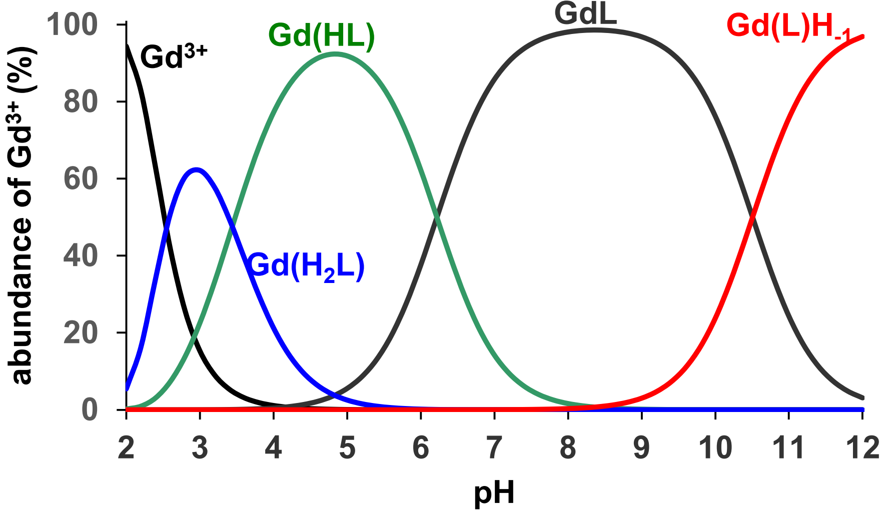

Figure S4. Species distribution of the Gd^{3+} - AAZ3A-endoHB system ($[Gd^{3+}]$=[AAZ3A-endoHB]=1.0 mM, 0.15 M NaCl, 25 °C)

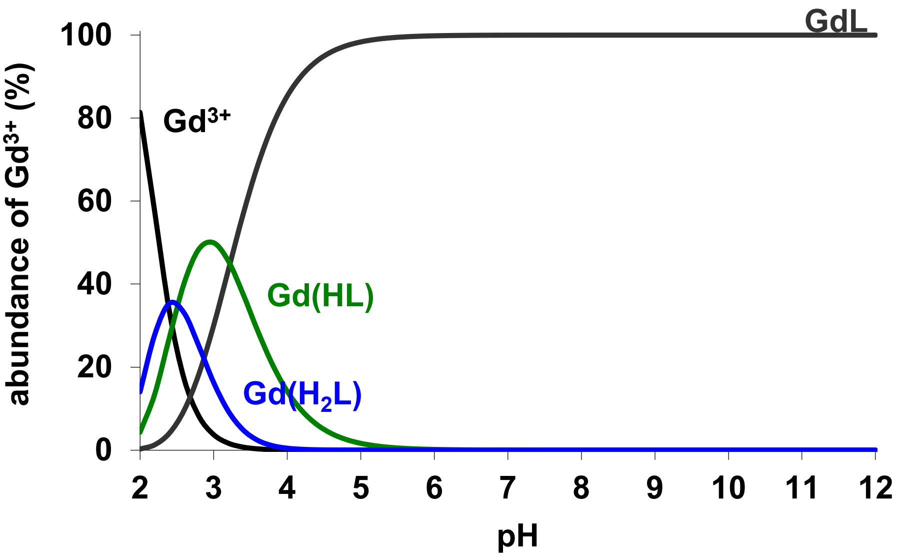

Figure S5. Species distribution of the Gd^{3+} - AAZ3A-exoHB system ($[Gd^{3+}]$=[AAZ3A-endoHB]=1.0 mM, 0.15 M NaCl, 25 °C).

1.2. Kinetic inertness of Gd(AAZ3A-endoHB) and Gd(AAZ3A-exoHB)

The kinetic inertness of Gd(AAZ3A-endoHB) and Gd(AAZ3A-exoHB) was determined by following the transmetallation reaction between the Gd(III)-complexes and Cu^{2+} ion (Equation S4) with spectrophotometry on the absorption band of the resulting Cu^{II}-complexes in the presence of Cu^{2+} excess in the pH range 2.8 – 5.0.

$$GdL + Cu^{2+} \rightleftharpoons CuL + Gd^{3+} \qquad (S4)$$

Some characteristic absorption spectra of the Gd(AAZ3A-endoHB) – Cu^{2+} and Gd(AAZ3A-exoHB) – Cu^{2+} reacting systems are shown in Figures S6 and S7.

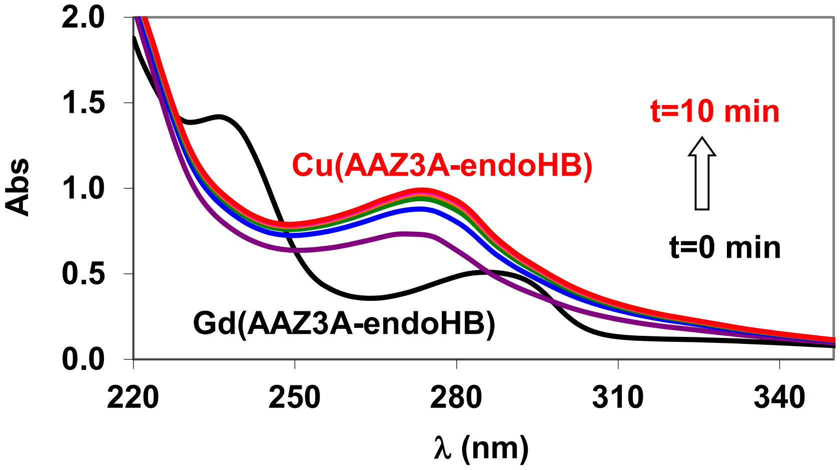

Figure S6. Absorption spectra of Gd(AAZ3A-endoHB) – Cu^{2+} reacting system ([GdL]=0.2 mM, $[Cu^{2+}]$=2.0 mM, [DMP]=0.01 M, pH=4.0, l=0.874 cm, 0.15 NaCl, 25 °C)

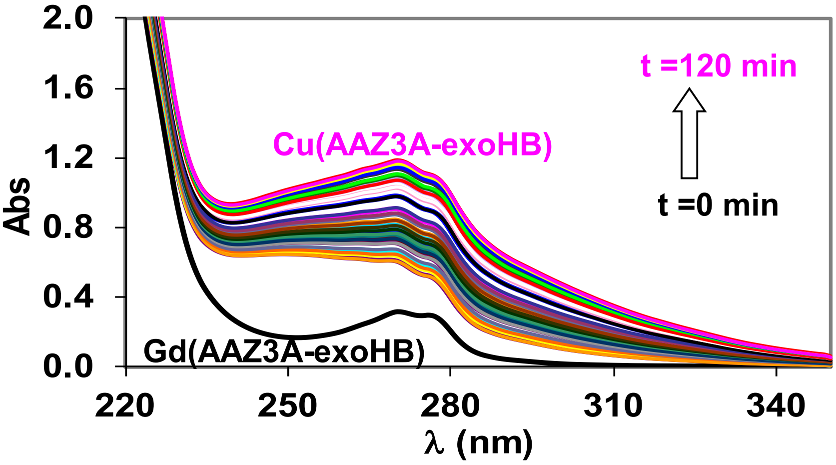

Figure S7. Absorption spectra of Gd(AAZ3A-exoHB) – Cu^{2+} reacting system ([GdL]=0.2 mM, [Cu^{2+}]=2.0 mM, [NMP]=0.01 M, pH=4.0, l=0.874 cm, 0.15 NaCl, 25 °C

In the presence of excess of the exchanging ion, the transmetallation can be treated as a pseudo-first-order process and the reaction rates can be expressed with the Equation S5, where k_d is a pseudo-first-order rate constant and $[GdL]_{tot}$ is the total concentration of the complex.

$$-\frac{d[GdL]_{tot}}{dt} = k_d[GdL]_{tot} \qquad (S5)$$

The rates of the transmetallation reactions were studied at different concentrations of the exchanging Cu^{2+} ion in the pH range 2.8 – 5.0. The obtained rate constants k_d characterizing the transmetallation reactions of Gd(AAZ3A-endoHB) and Gd(AAZ3A-exoHB) with Cu^{2+} are presented as a function of [H^+] and pH in Figures S8 and S9.

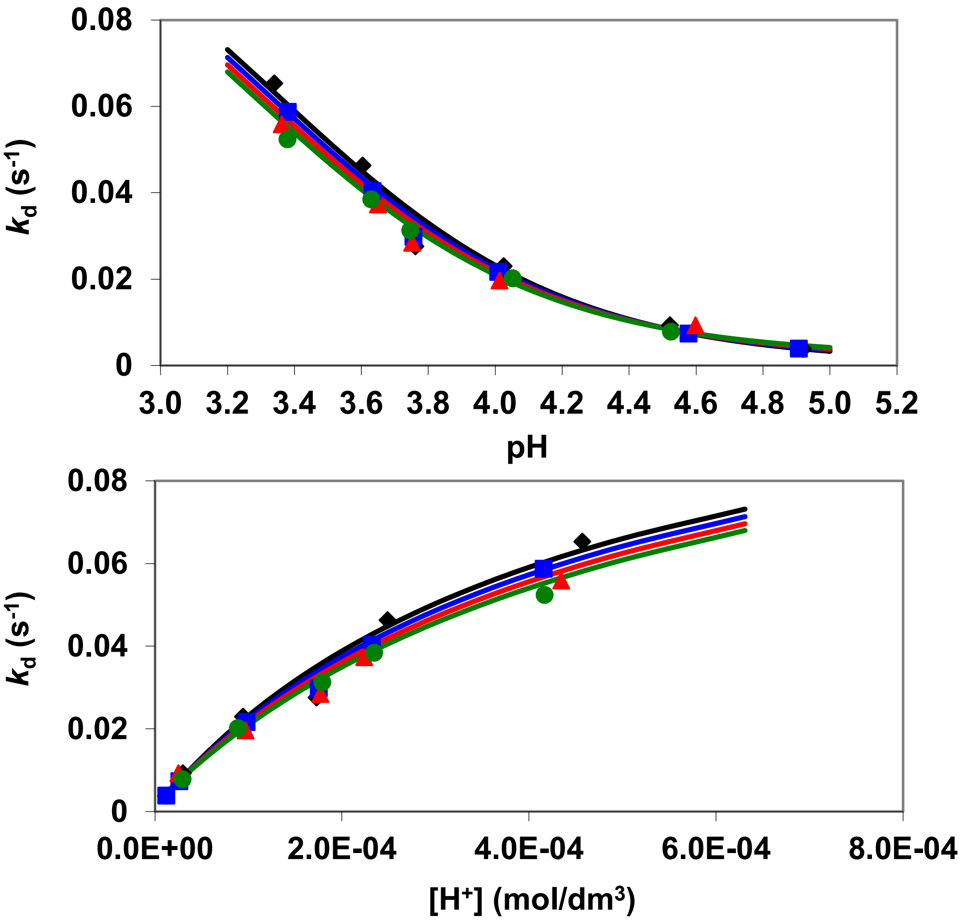

Figure S8. k_d pseudo-first-order rate constant characterizing the transmetallation reaction between Gd(AAZ3A-endoHB) and Cu^{2+} ([GdL]=0.2 mM, [Cu^{2+}]=2.0 mM (🕘), 4.0 mM (○), 6.0 mM (☐) and 8.0 mM (❦), [NMP]=[DMP]=[MKE]=0.01 M, 0.15 M NaCl, 25 °C)

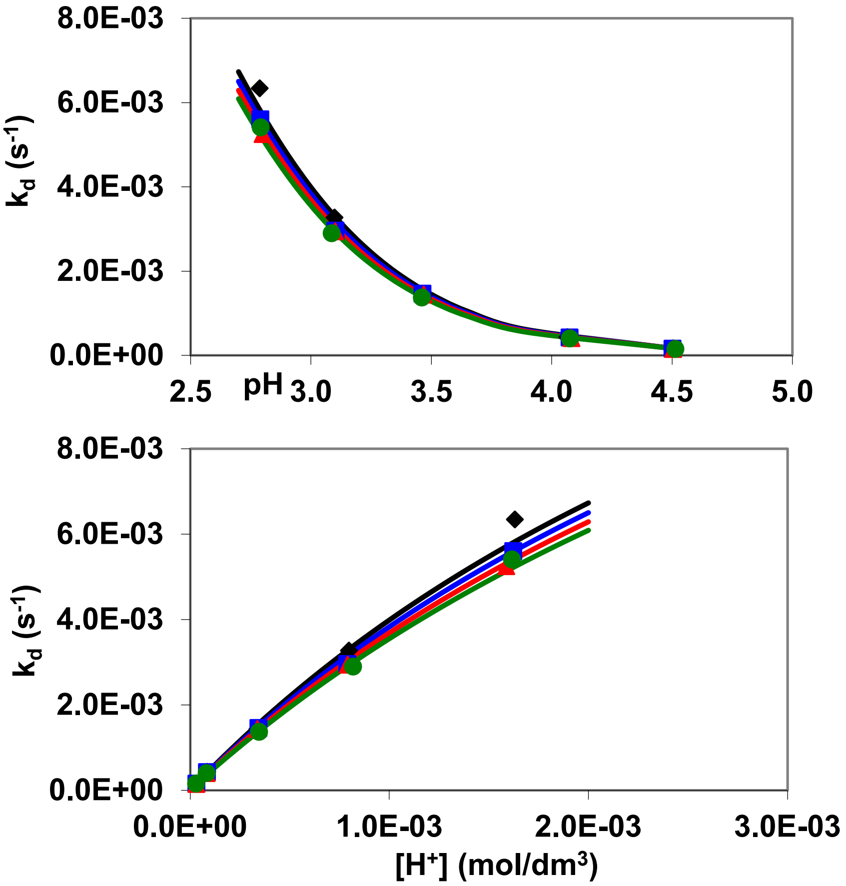

Figure S9. k_d pseudo-first-order rate constant characterizing the transmetallation reaction between Gd(AAZ3A-exoHB) and Cu^{2+} ([GdL]=0.2 mM, [Cu^{2+}]=2.0 mM (🕘), 4.0 mM (○), 6.0 mM (□) and 8.0 mM (℘), [NMP]=[DMP]=[MKE]=0.01 M, 0.15 M NaCl, 25 °C)

The k_d values increase with increase of [H^+], (particularly at lower [Cu^{2+}]) and decrease with increasing [Cu^{2+}] at pH < 4.0. The increase in the k_d values with increasing [H^+] can be interpreted in terms of the relatively slow proton assisted dissociation of Gd(III)-complexes, followed by a fast reaction between the free ligands and the exchanging metal ions Cu^{2+}. The k_d vs. [H^+] data can be expressed as a first-order function of [H^+] which can be interpreted by proton assisted (Equation S6) pathways. The proton assisted dissociation of the Gd(III)-complexes can occur by the equilibrium formation of a diprotonated GdH_2L complex ($K_{Gd(H2L)}$=[$Gd(H_2L)$]/[Gd(HL)][H^+]), which slowly dissociates and the free ligand rapidly reacts with the exchanging metal ions (Gd(HL) species predominates at pH<4.0).

$$Gd(H_2L) \xrightarrow{k_{GdH2L}} Gd^{3+} + H_xL \qquad (S6)$$

The transmetallation reaction can also take place with the direct attack of the exchanging metal ion on the Gd(III)-complex, via the formation of dinuclear intermediate (Equation S7). The formation of dinuclear [Lu(AAZTA)]Cu complex was also observed by ^{1}H-NMR spectroscopy in the presence of the large excess of the Cu^{2+}-ion.[2] It can be assumed that in the dinuclear intermediate Gd(L)Cu, the functional groups of the ligand are slowly transferred from the Gd^{3+} to the attacking Cu^{2+} step by step (Equation S8).

$$\mathrm{GdL} + \mathrm{Cu}^{2+} \overset{K_{\mathrm{GdLCu}}}{\rightleftharpoons} \mathrm{Gd(L)Cu} \qquad (S7)$$

$$K_{GdLCu} = \frac{[Gd(L)Cu]}{[GdL][Cu^{2+}]}$$

$$\mathrm{Gd(L)Cu} \xrightarrow{k_{\mathrm{GdLCu}}} \mathrm{Gd}^{3+} + \mathrm{CuL} \qquad (S8)$$

The k_d *vs*. [H^+] graphs in Figures S8 and S9 reveal that the increase of [Cu^{2+}] results in a slight decrease in the k_d values at higher lower pH values. This phenomenon can be interpreted by considering that the larger concentration of the exchanging metal ion results in the formation of dinuclear species which reduces the concentration of the kinetically more active protonated $\mathrm{GdH_2L}$ species and the contribution of the proton-assisted dissociation to the overall dissociation rate of the Gd(III)-complexes ([Cu^{2+}]>>[H^+]). Similar phenomena were identified in the kinetic studies of the transmetallation reaction of Gd(AAZTA) and Gd(DTPA) complexes.[2,4] By taking into account all possible pathways, the rate of the transmetallation of Gd(III)-complexes can be expressed by Equation S9, where the [GdHL], [$\mathrm{GdH_2L}$] and [GdLM] are the concentrations of the protonated and dinuclear complexes, respectively:

$$-\frac{[GdL]_{tot}}{dt} = k_{GdH2L}[GdH2L] + k_{GdLCu}[GdLCu] \qquad (S9)$$

If we take into account the total concentration of the Gd(III)-complexes ($[\mathrm{GdL}]_\mathrm{tot}$=[GdHL]+[$\mathrm{GdH_2L}$]+[Gd(L)Cu]), the definition of the protonation constant for the formation of the diprotonated Gd(III)-complexes, the stability constant of the dinuclear Gd(L)Cu complex (Equation S7) and Equation S5, the pseudo-first-order rate constant can be expressed as follows:

$$k_d = \frac{k_1[H^+] + k_3[Cu^{2+}]}{1 + K^H_{GdH2L}[H^+] + K_{GdLCu}[Cu^{2+}]} \qquad (S10)$$

The rate constants, $k_1 = k_{\mathrm{GdH2L}} \times K^{\mathrm{H}}_{\mathrm{GdH2L}}$ and $k_3 = k_{\mathrm{GdLCu}} \times K_{\mathrm{GdLCu}}$ are characteristic of the spontaneous, proton- and metal-assisted dissociation of the Gd(III)-complexes, respectively. The rate, protonation and stability constants were calculated by fitting the k_d values in Figures S8 and S9 to the Equation S10.

2. Relaxometry

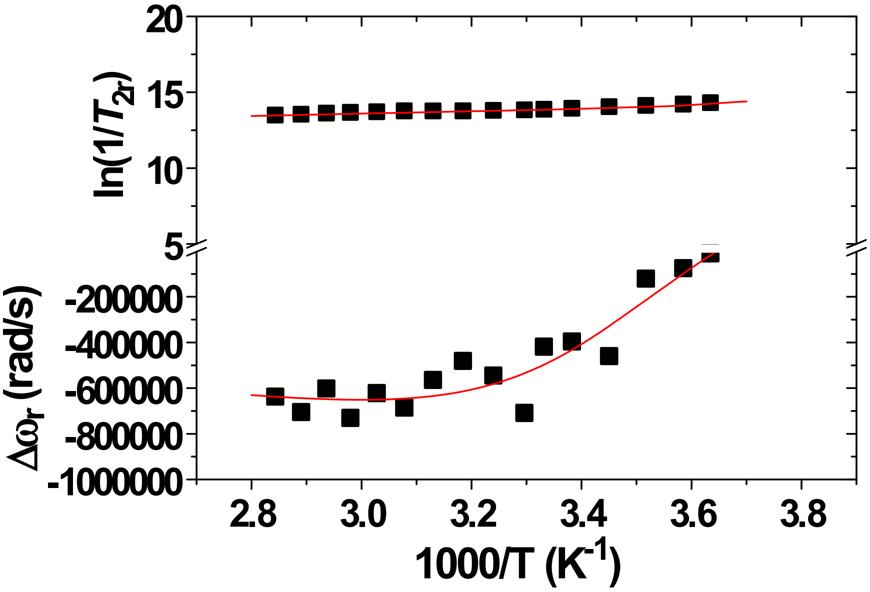

Figure S10. Reduced transverse ^{17}O relaxation rates (*top*) and chemical shifts (*bottom*) measured at 11.74 T (pH 7) for Gd(AAZ3A-endoHB) The solid lines correspond to the fits of the data as described in the main text.

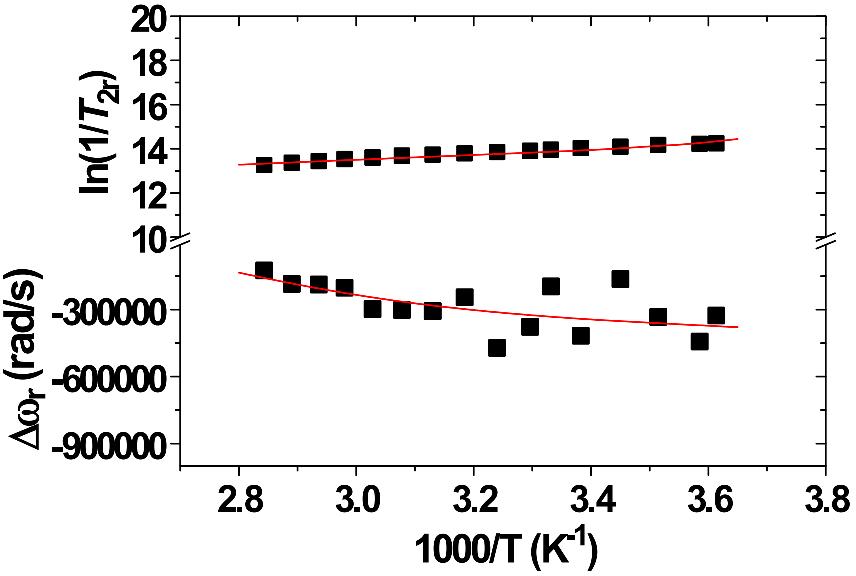

Figure S11. Reduced transverse ^{17}O relaxation rates (top) and chemical shifts (bottom) measured at 11.74 T (pH 7) for Gd(AAZ3A-exoHB) The solid lines correspond to the fits of the data as described in the main text.

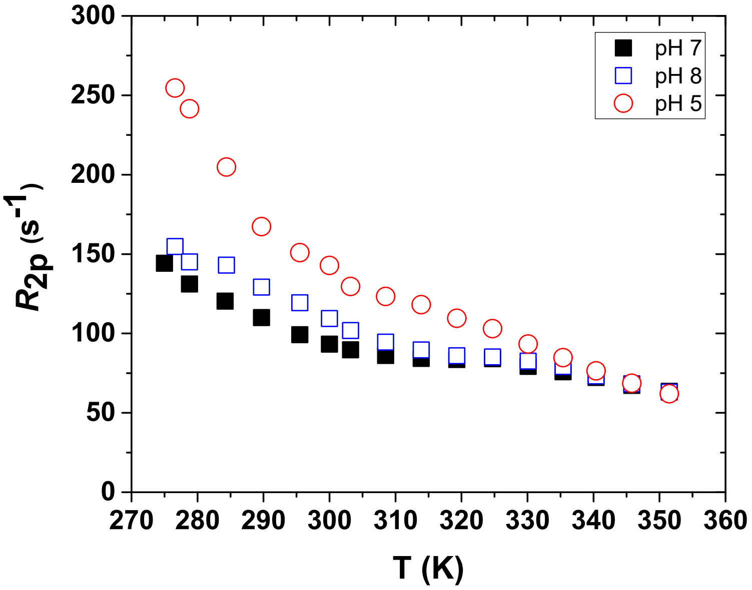

Figure S12. ^{17}O NMR transverse relaxation rates as a function of temperature measured at pH 5.0, 7.0 and 8.0 and 500 MHz (11.74 T) for Gd(AAZ3A-endoHB).

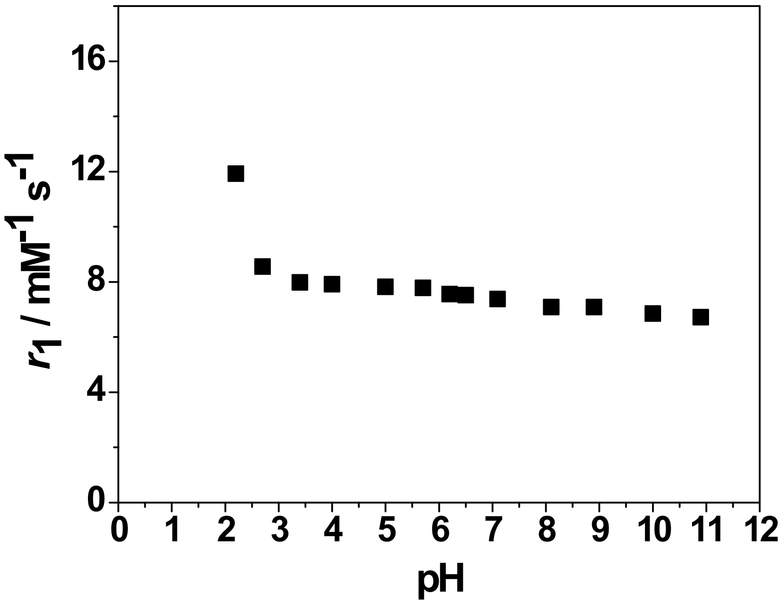

Figure S13. Variation of the longitudinal water proton relaxivity of Gd(AAZ3A-endoHB) at 20 MHz, 298 K as a function of pH.

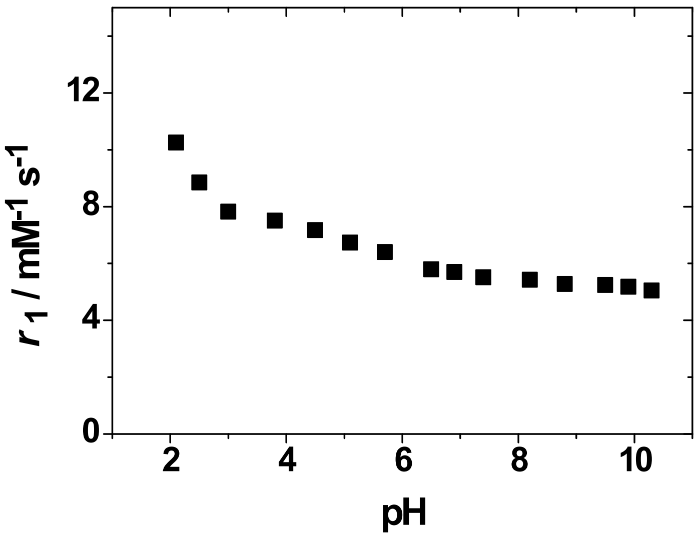

Figure S14. Variation of the longitudinal water proton relaxivity of Gd(AAZ3A-exoHB) at 20 MHz, 298 K as a function of pH.

3. VT-^{1}H NMR studies of the Eu(AAZ3A-endoHB)

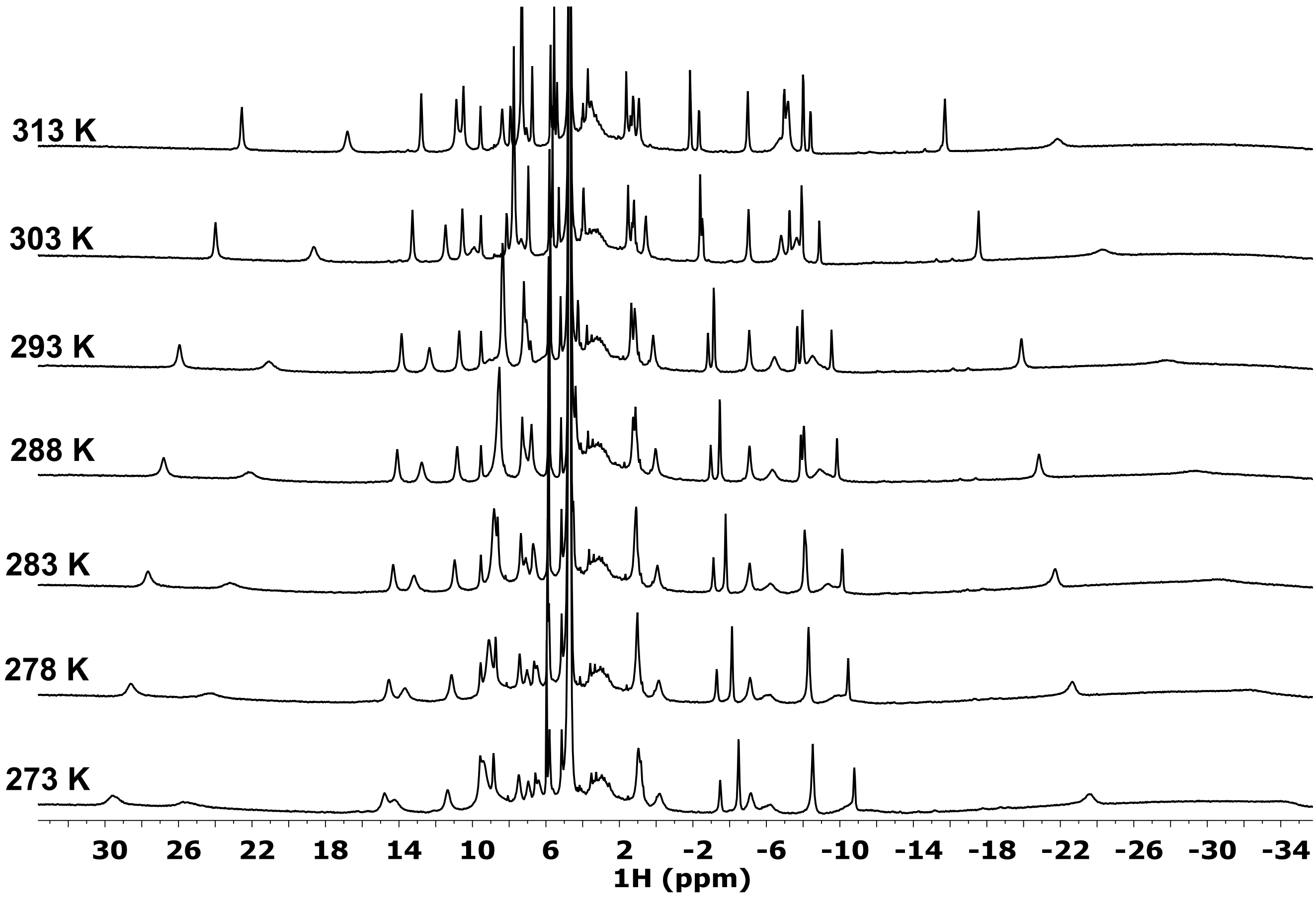

Figure S15. VT-^{1}H NMR spectra of the Eu(AAZ3A-endoHB) ([EuL] = 5.0 mM, pD = 7.4)

^1H NMR measurements were performed with the Bruker Avance III (9.39 T) spectrometer, equipped with Bruker Variable Temperature Unit (BVT), Bruker Cooling Unit (BCU) and a BB inverse *z* gradient probe (5 mm). For the VT- NMR measurements 5.0 mM solution of Eu(AAZ3A-endoHB) was prepared at pD=7.4 in D_2O. The pH was adjusted by stepwise addition of concentrated NaOD and DCl solutions. The chemical shifts are reported in ppm, relative to DSS for ^1H as the external standard. The signals are related to each proton of the ligand backbone, except for the three methyl protons in position 6 which present one single peak. The rigidity of the Eu-complex is responsible for the differentiation of each proton as already shown in case of Eu(CyAAZTA).[3]

4. Theoretical calculations

Table S1. Optimized Cartesian coordinates obtained for $[Gd(AAZ3A\text{-}endoHB)(H_2O)_2]^-\cdot 4H_2O$.

Center Number	Atomic Number	Coordinates (Angstroms) X	Y	Z
1	64	-0.453088	-0.275481	-0.382778
2	7	0.704044	1.693318	1.059868
3	6	-0.141447	2.908337	0.990623
4	1	0.475416	3.802594	0.871560
5	1	-0.708637	3.042082	1.911158
6	7	-1.284484	-0.079480	2.204943
7	6	-1.185431	2.855757	-0.134278
8	7	1.147691	-1.223492	1.619924
9	6	0.894641	1.160726	2.446080
10	6	1.740493	-0.117264	2.397119
11	1	2.719186	0.112096	1.983194
12	1	1.918637	-0.441500	3.430922
13	6	0.261898	-2.038524	2.479785
14	1	0.736649	-2.172349	3.460063
15	1	0.175057	-3.021511	2.020244
16	8	-1.420807	3.879290	-0.784000
17	8	-1.762145	1.735620	-0.285603
18	6	-1.162577	-1.477515	2.640928
19	1	-1.483705	-1.578806	3.687038
20	1	-1.843059	-2.063191	2.024506
21	8	0.762547	1.443257	-1.639986
22	6	-0.478224	0.817390	3.050311
23	1	-0.308013	0.366838	4.035852
24	1	-1.042152	1.728947	3.242071
25	8	2.354142	3.005127	-1.788200
26	6	1.953268	1.990340	0.336379
27	1	2.644878	1.149648	0.396317
28	1	2.458883	2.877386	0.730770
29	8	-0.824214	-2.765680	-0.378911

30	6	1.685284	2.191897	-1.160990
31	6	2.226320	-2.110469	1.101988
32	1	1.722807	-2.934214	0.593277
33	1	2.795800	-2.528165	1.944271
34	8	-2.740994	-0.904962	0.122364
35	8	-4.618914	0.078170	0.779016
36	6	1.600088	2.161858	3.368481
37	1	2.619492	2.357383	3.029024
38	1	1.062917	3.112159	3.403390
39	6	-2.695838	0.321859	2.167624
40	1	-2.753688	1.407826	2.108045
41	1	-3.238822	0.005734	3.069014
42	6	-3.428152	-0.203912	0.935343
43	8	-1.754535	-0.206287	-2.534315
44	1	1.655245	1.770996	4.387049
45	1	-1.636867	0.696805	-2.901972
46	1	-2.712731	-0.257706	-2.331292
47	1	-0.221365	-3.345498	-0.883566
48	1	-1.731017	-3.108281	-0.494837
49	8	1.062552	-3.915663	-1.939991
50	1	1.315584	-2.962943	-1.871353
51	1	1.777980	-4.403228	-1.528124
52	8	-3.484427	-3.295433	-0.788124
53	1	-3.922038	-3.747949	-0.064595
54	1	-3.475811	-2.352134	-0.528040
55	8	-4.514764	-0.104075	-2.075175
56	8	-1.156122	2.387425	-3.288690
57	1	-4.818238	0.756527	-2.370120
58	1	-4.615140	-0.085476	-1.104219
59	1	-1.545458	2.930665	-2.585113
60	1	-0.299842	2.148032	-2.881432
61	6	3.152964	-1.423645	0.140724
62	6	2.651482	-1.068967	-1.132987
63	6	4.470169	-1.123882	0.477213
64	6	3.514318	-0.415803	-2.027983
65	6	5.310984	-0.465762	-0.413285
66	1	4.837456	-1.403405	1.461018
67	6	4.819740	-0.114757	-1.668636
68	1	3.125681	-0.131139	-2.999014
69	1	6.331453	-0.231423	-0.133922
70	1	5.460643	0.404147	-2.374147
71	8	1.398906	-1.347859	-1.448265

E(RwB97XD) = -1923.7885969 Hartree
Zero-point correction = 0.578505
Thermal correction to Energy = 0.619422
Thermal correction to Enthalpy = 0.620366
Thermal correction to Gibbs Free Energy = 0.509131
Sum of electronic and zero-point Energies = -1923.210092
Sum of electronic and thermal Energies = -1923.169175

Sum of electronic and thermal Enthalpies = -1923.168231
Sum of electronic and thermal Free Energies = -1923.279466

Table S2. Optimized Cartesian coordinates obtained for $[Gd(AAZ3A\text{-}endoHB)(H_2O)_2]^{-}\cdot 5H_2O$.

Center Number	Atomic Number	Atomic Type	Coordinates (Angstroms) X	Y	Z
1	64		0.441865	0.120991	-0.355062
2	7		-0.897416	-1.769015	0.934880
3	6		-0.235168	-3.080761	0.719884
4	1		-0.965164	-3.825047	0.396665
5	1		0.197449	-3.468186	1.641839
6	7		1.302344	-0.267824	2.226292
7	6		0.906507	-3.037482	-0.305296
8	7		-0.996514	1.126165	1.696132
9	6		-0.966411	-1.338396	2.369267
10	6		-1.636031	0.045736	2.475443
11	1		-2.674457	-0.038551	2.156949
12	1		-1.666281	0.321711	3.537609
13	6		-0.003165	1.864969	2.503751
14	1		-0.486699	2.270830	3.402569
15	1		0.329758	2.708436	1.894587
16	8		1.110240	-4.033167	-1.003862
17	8		1.582385	-1.960410	-0.338141
18	6		1.232621	1.039471	2.898592
19	1		1.274980	0.894951	3.985351
20	1		2.115666	1.609928	2.614340
21	8		-0.929402	-1.349149	-1.718864
22	6		0.465568	-1.257729	2.920497
23	1		0.404339	-1.027454	3.991363
24	1		0.946660	-2.231130	2.850749
25	8		-2.757834	-2.614265	-1.950777
26	6		-2.193512	-1.817864	0.232268
27	1		-2.742496	-0.885705	0.369372
28	1		-2.824312	-2.641117	0.580390
29	8		1.478035	4.193288	0.358105
30	6		-1.968841	-1.963153	-1.280009
31	6		-2.013191	2.125994	1.268444
32	1		-1.454121	2.970880	0.862236
33	1		-2.568166	2.482577	2.146966
34	8		2.659525	0.792662	0.233701
35	8		4.567484	-0.256341	0.671977
36	6		-1.776918	-2.311119	3.234433
37	1		-2.810970	-2.372937	2.889416
38	1		-1.349587	-3.315723	3.213786
39	6		2.699332	-0.695261	2.097707

40	1		2.728769	-1.761006	1.875654
41	1		3.279304	-0.522463	3.013494
42	6		3.388552	-0.003040	0.922476
43	8		1.697174	0.083355	-2.515933
44	1		-1.790304	-1.976732	4.274044
45	1		1.556680	-0.794786	-2.932132
46	1		2.665079	0.166268	-2.381665
47	1		0.698757	4.250449	-0.220745
48	1		2.177509	3.862550	-0.224238
49	8		-0.674780	4.185392	-1.398821
50	1		-0.849010	3.215966	-1.420049
51	1		-1.504710	4.583290	-1.131059
52	8		3.596446	2.944064	-1.067389
53	1		3.917412	2.574154	-1.893844
54	1		3.359252	2.143478	-0.559161
55	8		4.411040	0.319940	-2.093099
56	8		0.920577	-2.397588	-3.406343
57	1		4.978844	-0.277159	-2.583011
58	1		4.575278	0.134765	-1.146580
59	1		1.259347	-3.025810	-2.749458
60	1		0.084971	-2.113194	-2.987491
61	6		-2.959675	1.624466	0.219933
62	6		-2.445435	1.381253	-1.073690
63	6		-4.309060	1.411034	0.484896
64	6		-3.328748	0.934722	-2.067155
65	6		-5.171199	0.948920	-0.503241
66	1		-4.685724	1.604722	1.485442
67	6		-4.668648	0.715733	-1.780785
68	1		-2.933411	0.741663	-3.057841
69	1		-6.217981	0.777237	-0.281976
70	1		-5.327617	0.353124	-2.562826
71	8		-1.152991	1.556769	-1.314605

E(RwB97XD) = -1923.7835273 Hartree
Zero-point correction = 0.578200
Thermal correction to Energy = 0.619698
Thermal correction to Enthalpy = 0.620642
Thermal correction to Gibbs Free Energy = 0.506567
Sum of electronic and zero-point Energies = -1923.205327
Sum of electronic and thermal Energies = -1923.163829
Sum of electronic and thermal Enthalpies = -1923.162885
Sum of electronic and thermal Free Energies= -1923.276960

Table S3. Optimized Cartesian coordinates obtained for $[Gd(AAZ3A\text{-}exoHB)(H_2O)_2]^{-}\cdot 4H_2O$.

Center Number	Atomic Number	Atomic Type	Coordinates (Angstroms)		
			X	Y	Z
1	64		0.373755	0.302502	-0.213956

2	8	1.139602	1.993638	1.366826
3	7	-1.551507	-1.348324	0.807153
4	6	-2.289742	-1.995999	-0.289949
5	1	-3.324665	-2.215525	-0.014732
6	1	-1.831670	-2.951725	-0.541245
7	8	2.446381	2.466977	3.104053
8	7	1.125616	-2.293475	0.112512
9	6	-2.288874	-1.211411	-1.607912
10	7	0.913406	-0.611229	2.293686
11	6	-0.840156	-2.329214	1.692680
12	6	-0.086641	-1.575647	2.795081
13	1	-0.800516	-1.046395	3.422988
14	1	0.396532	-2.317132	3.443888
15	6	2.238313	-1.249087	2.128128
16	1	2.470206	-1.832618	3.027765
17	1	2.974796	-0.449250	2.054148
18	8	-3.165098	-1.455179	-2.430568
19	8	-1.305116	-0.409887	-1.775836
20	6	2.381151	-2.126782	0.866696
21	1	2.780527	-3.112003	1.140197
22	1	3.101337	-1.650612	0.202356
23	6	0.177304	-3.130051	0.867812
24	1	0.720005	-3.790774	1.554741
25	1	-0.338415	-3.794068	0.176452
26	6	-2.490405	-0.471622	1.571688
27	1	-1.898105	0.171117	2.225164
28	1	-3.148529	-1.083499	2.198370
29	8	2.901944	0.682499	-0.208024
30	6	1.049898	0.524052	3.221989
31	1	1.666566	0.267256	4.090203
32	1	0.057064	0.803592	3.582767
33	8	1.523566	-0.705013	-2.121528
34	6	1.610453	1.764427	2.522552
35	8	2.990330	-2.198467	-2.873552
36	6	-1.781876	-3.339193	2.365875
37	1	-2.443592	-2.861418	3.089765
38	1	-2.396957	-3.855887	1.626447
39	6	1.421251	-2.885042	-1.200079
40	1	0.479190	-3.194049	-1.660051
41	1	2.069488	-3.764647	-1.114144
42	6	2.047230	-1.861058	-2.147799
43	8	0.781972	2.169855	-1.829656
44	1	-1.201168	-4.093132	2.902028
45	1	0.428355	3.011082	-1.482221
46	1	0.402312	1.964014	-2.704664
47	1	3.206125	1.548576	0.129041
48	1	3.366213	0.537482	-1.056342
49	8	3.842436	3.101392	0.797428
50	1	4.768303	3.038593	1.038867
51	1	3.355316	3.060219	1.644551

52	8		4.349117	0.203770	-2.540153
53	1		3.900581	-0.613003	-2.834544
54	1		5.240958	-0.070121	-2.318581
55	8		-0.077999	0.683141	-3.943219
56	8		-0.106302	4.039685	-0.062278
57	1		0.696027	0.175084	-3.654847
58	1		-0.757844	0.300340	-3.354608
59	1		0.580684	3.687575	0.523701
60	1		-0.791523	3.345657	0.056440
61	6		-3.343583	0.415404	0.708431
62	6		-2.738863	1.519790	0.068001
63	6		-4.709021	0.191587	0.563822
64	6		-3.554603	2.367229	-0.703881
65	6		-5.504545	1.030089	-0.208973
66	1		-5.156297	-0.662637	1.065162
67	6		-4.912530	2.121347	-0.841335
68	1		-3.091764	3.214833	-1.199665
69	1		-6.565713	0.837623	-0.315079
70	1		-5.516497	2.787275	-1.449793
71	8		-1.450684	1.735882	0.200034

E(RwB97XD) = -1923.7868873
Zero-point correction = 0.579590 (Hartree/Particle)
Thermal correction to Energy = 0.620283
Thermal correction to Enthalpy = 0.621227
Thermal correction to Gibbs Free Energy = 0.510468
Sum of electronic and zero-point Energies = -1923.207297
Sum of electronic and thermal Energies = -1923.166604
Sum of electronic and thermal Enthalpies = -1923.165660
Sum of electronic and thermal Free Energies = -1923.276419

Table S4. Optimized Cartesian coordinates obtained for [Gd(AAZ3A-exoHB)(H_2O)]$^{-}\cdot 5H_2O$.

Center Number	Atomic Number	Atomic Type	Coordinates (Angstroms) X	Y	Z
1	64		-0.361178	0.133537	0.235639
2	8		-1.569534	1.873991	-0.897462
3	7		1.458083	-1.450687	-0.934228
4	6		2.082586	-2.300709	0.094879
5	1		3.099997	-2.592383	-0.180558
6	1		1.519894	-3.225988	0.216248
7	8		-1.617116	3.228261	-2.667266
8	7		-1.321460	-2.235537	-0.459225
9	6		2.114855	-1.677182	1.496556
10	7		-0.865003	-0.290747	-2.342617
11	6		0.701049	-2.226885	-1.976886
12	6		0.067325	-1.247240	-2.973967
13	1		0.842724	-0.696021	-3.500702

14	1	-0.453627	-1.834237	-3.739084
15	6	-2.244061	-0.827630	-2.345079
16	1	-2.447123	-1.296082	-3.314448
17	1	-2.934719	0.007644	-2.236406
18	8	2.936204	-2.087794	2.303036
19	8	1.196947	-0.809044	1.737293
20	6	-2.530987	-1.810449	-1.191683
21	1	-3.065631	-2.689766	-1.572029
22	1	-3.190249	-1.307696	-0.479347
23	6	-0.426654	-3.037581	-1.313803
24	1	-1.002080	-3.525263	-2.109385
25	1	-0.006853	-3.848716	-0.721173
26	6	2.521686	-0.594123	-1.538085
27	1	2.049252	0.092448	-2.238127
28	1	3.227758	-1.220041	-2.094952
29	8	-4.151379	0.989841	-0.116006
30	6	-0.834726	1.017021	-3.009645
31	1	-1.360672	1.006575	-3.971504
32	1	0.205010	1.289100	-3.206438
33	8	-1.816552	-0.891853	1.875804
34	6	-1.401249	2.138372	-2.133984
35	8	-3.243824	-2.480274	2.518396
36	6	1.581342	-3.211714	-2.757746
37	1	2.312747	-2.695483	-3.381188
38	1	2.116303	-3.881333	-2.081076
39	6	-1.721745	-2.978869	0.743302
40	1	-0.826451	-3.410570	1.199134
41	1	-2.413644	-3.795479	0.508685
42	6	-2.344186	-2.067218	1.802035
43	8	-0.741589	1.787204	2.029835
44	1	0.963794	-3.826453	-3.416177
45	1	-0.334712	2.660446	1.822656
46	1	-0.447405	1.461812	2.899913
47	1	-3.313727	1.436649	-0.300356
48	1	-4.161581	0.876179	0.849342
49	8	-1.369187	5.178928	-0.757041
50	1	-0.896919	5.859847	-1.239621
51	1	-1.557497	4.487996	-1.426713
52	8	-3.979394	0.554910	2.675880
53	1	-4.484666	-0.234238	2.889456
54	1	-3.093286	0.179144	2.509724
55	8	-0.100755	-0.001926	3.998648
56	8	0.436969	3.901098	0.914644
57	1	-0.893847	-0.419258	3.635438
58	1	0.579841	-0.335277	3.383120
59	1	-0.208605	4.365894	0.346989
60	1	0.822985	3.201428	0.349464
61	6	3.286852	0.237051	-0.547822
62	6	2.644434	1.354363	0.026235
63	6	4.613167	-0.038329	-0.233594

64	6	3.380264	2.170910	0.900698
65	6	5.330879	0.767394	0.643282
66	1	5.090600	-0.903988	-0.684307
67	6	4.701873	1.875632	1.204500
68	1	2.888037	3.032605	1.339232
69	1	6.362393	0.536960	0.882157
70	1	5.246509	2.518070	1.889136
71	8	1.374620	1.601786	-0.252092

E(RwB97XD) = -1923.7897339
Zero-point correction = 0.579387
Thermal correction to Energy = 0.620559
Thermal correction to Enthalpy = 0.621503
Thermal correction to Gibbs Free Energy = 0.508392
Sum of electronic and zero-point Energies = -1923.210347
Sum of electronic and thermal Energies = -1923.169175
Sum of electronic and thermal Enthalpies = -1923.168231
Sum of electronic and thermal Free Energies = -1923.281342

Table S5. ZFS parameters obtained using CASSCF/NEVPT2 calculations.

	D / cm^{-1}	E/D	E	Δ / cm^{-1}	Δ^2 / rad^2s^{-2}
$[\mathrm{Gd(AAZ3A\text{-}endoHB)(H_2O)_2}]^{-}\cdot 4\mathrm{H_2O}$	-0.0544	0.2311	-0.01257	0.0478	8.1153×10^{19}
$[\mathrm{Gd(AAZ3A\text{-}exoHB)(H_2O)}]^{-}\cdot 5\mathrm{H_2O}$	0.05179	0.0807	0.004177	0.0427	6.4672×10^{19}

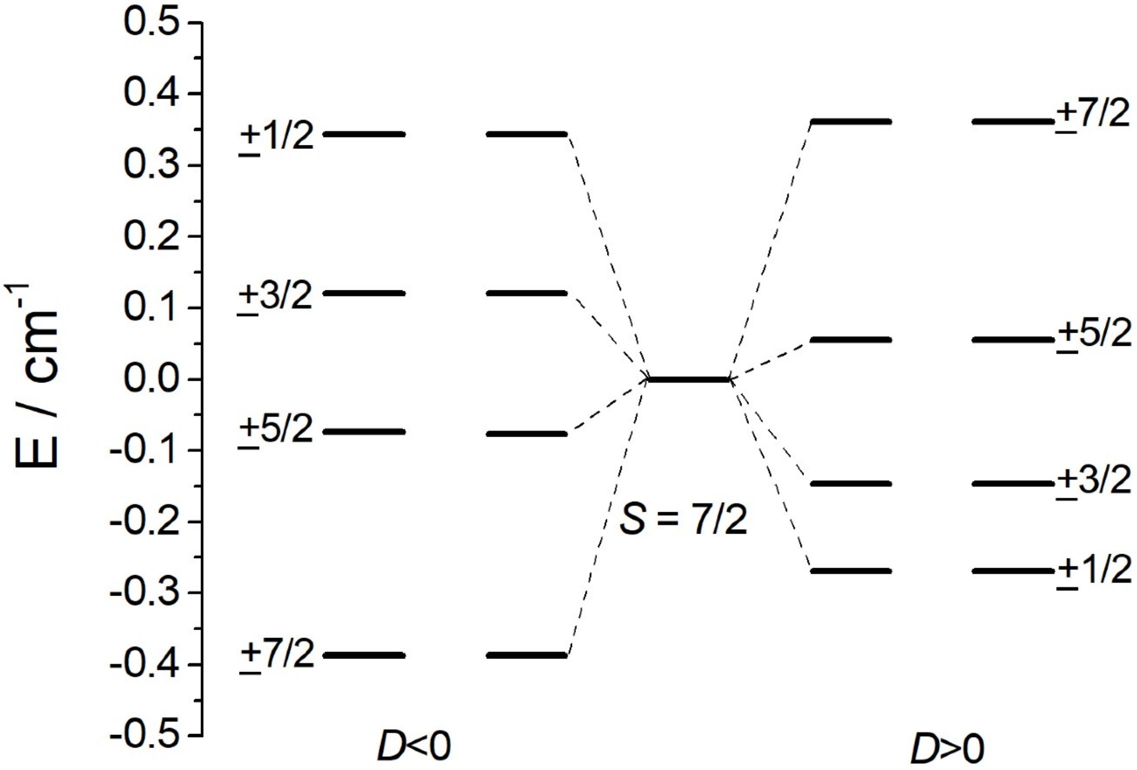

Figure S16. Energies of the Kramers doublets calculated for [Gd(AAZ3A-endoHB)(H_2O)$_2$]$^-$·4H_2O and [Gd(AAZ3A-exoHB)(H_2O)]$^-$·5H_2O at the CASSCF/NEVPT2 level.

5. HPLC-MS Methods and Chromatograms

5.1. AAZ3A-endoHB

Semi-preparative HPLC gradient conditions:

Solvent A: H_2O (TFA 0.1%); Solvent B: MeOH (TFA 0.1%); Flow: 20 mL/min; t_R = 9.2 min

Time (min)	Solvent A (%)	Solvent B (%)
0	99	1
2,00	99	1
8,50	56	44
9,50	0	100

Analytical HPLC gradient conditions:

Solvent A: H_2O (TFA 0.1%); Solvent B: MeOH (TFA 0.1%); Flow: 1 mL/min; t_R = 10.9 min

Time (min)	Solvent A (%)	Solvent B (%)
0	99	1
2,00	99	1
16,00	0	100
19,00	0	100

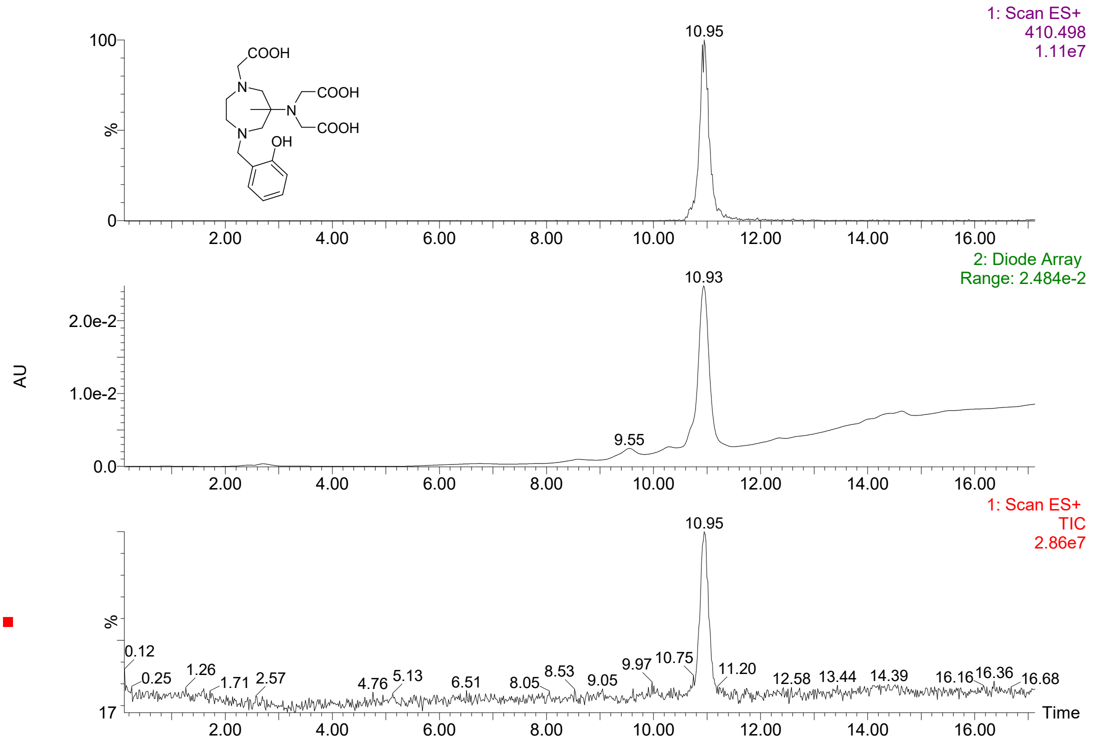

Figure S16. ESI^+ MS (*bottom*), UV (254 nm, *middle*) and specific ion ($M+H^+$, *top*) HPLC chromatograms of ligand AAZ3A-endoHB.

5.2. AAZ3A-exoHB

Analytical HPLC gradient conditions:

Solvent A: H_2O (TFA 0.1%); Solvent B: MeOH (TFA 0.1%); Flow: 1 mL/min; t_R = 11.7 min.

Time (min)	Solvent A (%)	Solvent B (%)
0	95	5
2,00	95	5
18,00	78	22
19,00	0	100

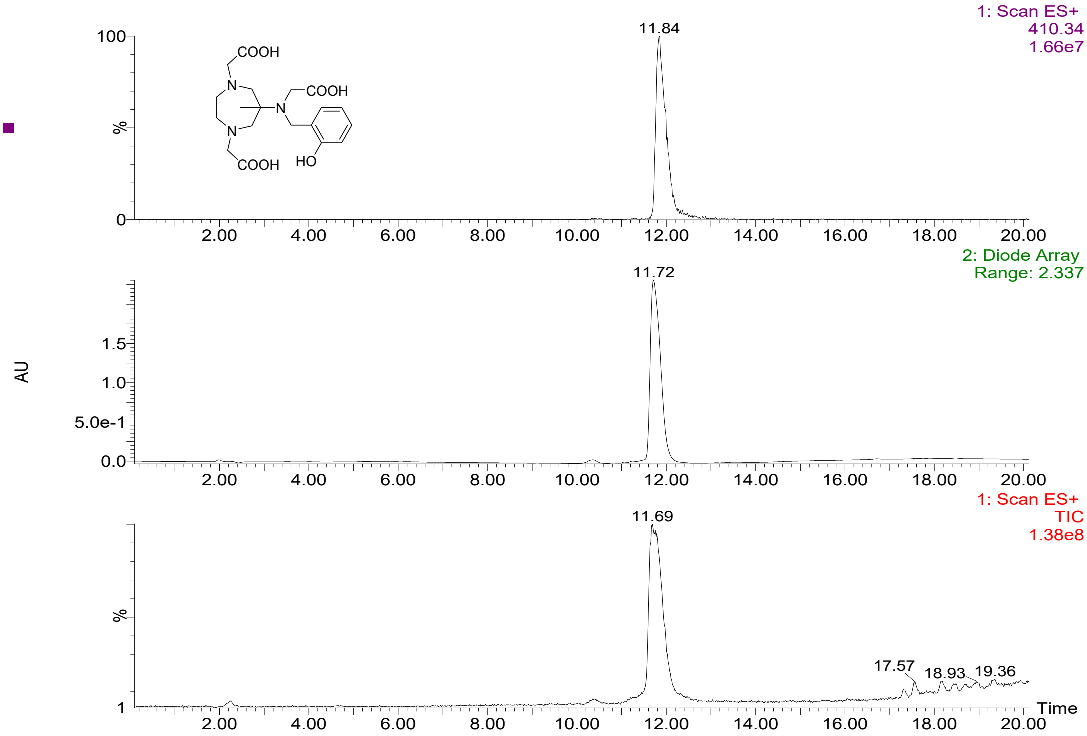

Figure S17. ESI$^+$ MS (*bottom*), UV (254 nm, *middle*) and specific ion (M+H$^+$, *top*) HPLC chromatograms of ligand AAZ3A-exoHB.

6. NMR Spectra

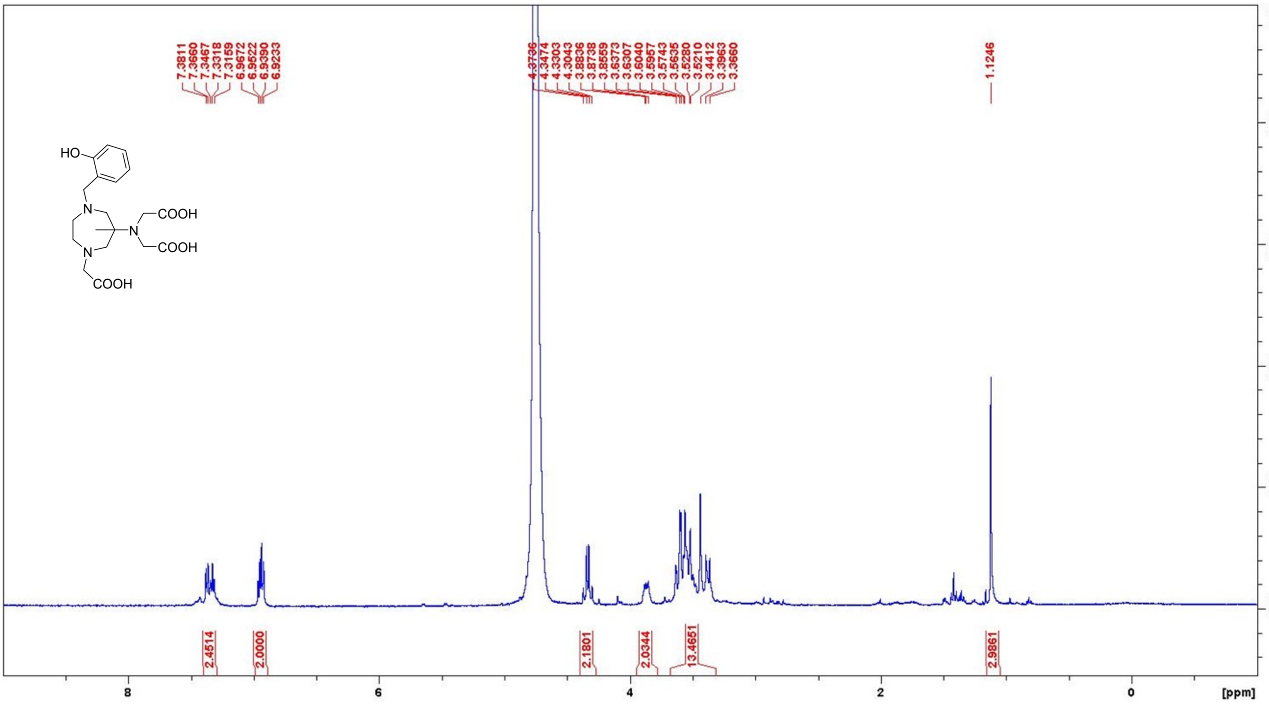

Figure S18. ^{1}H NMR spectrum in D_2O of ligand AAZ3A-endoHB.

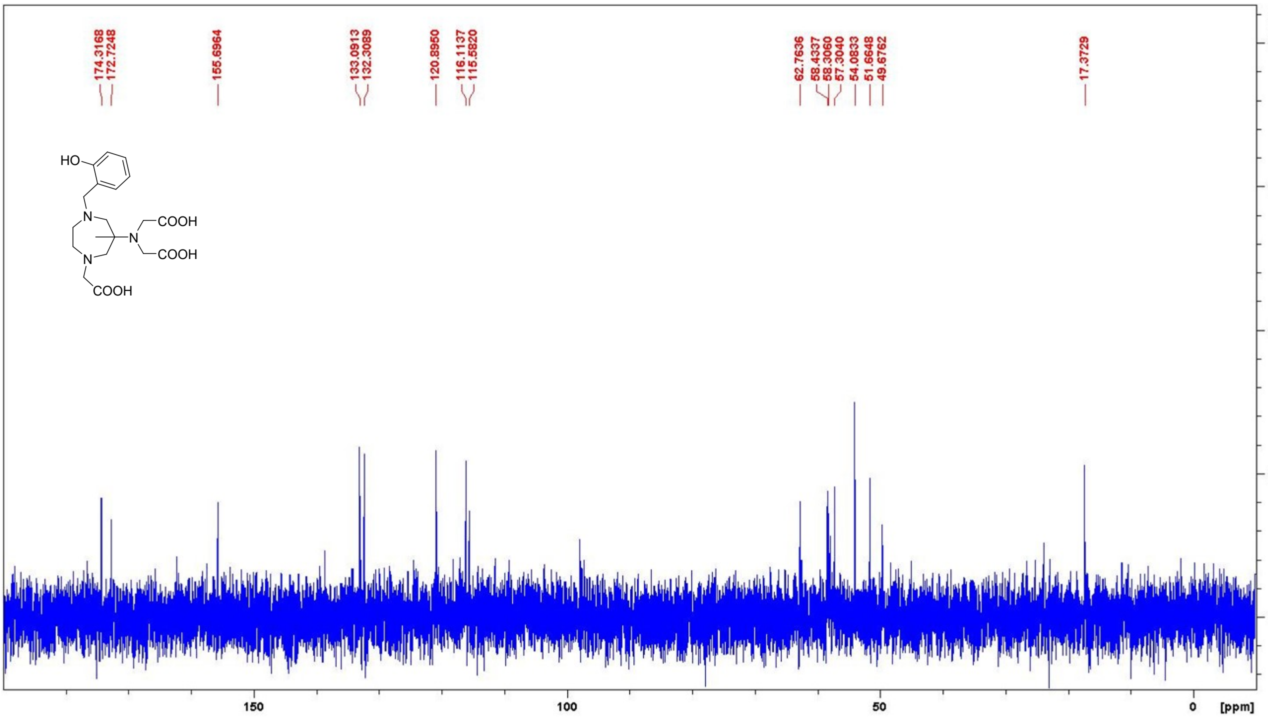

Figure S19. ^{13}C NMR spectrum in D_2O of ligand AAZ3A-endoHB.

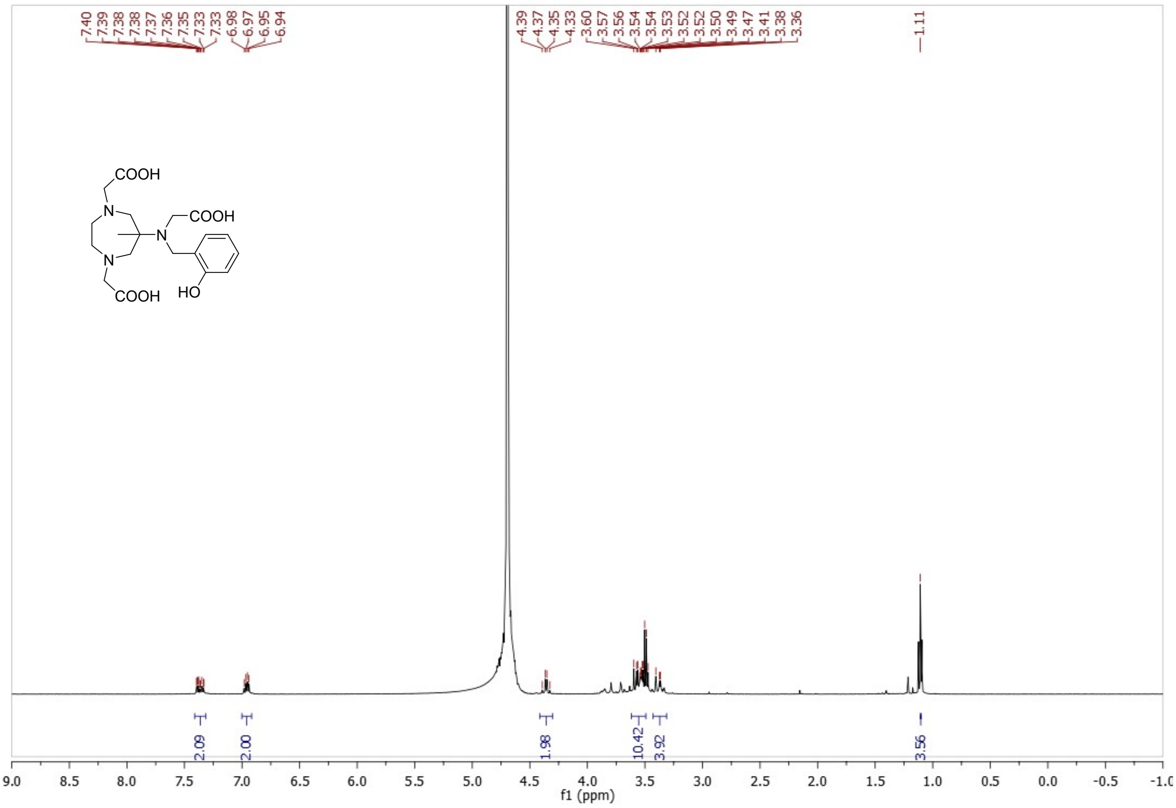

Figure S20. ^{1}H NMR spectrum in D_2O of ligand AAZ3A-exoHB (signals from residual Et_2O are also observable).

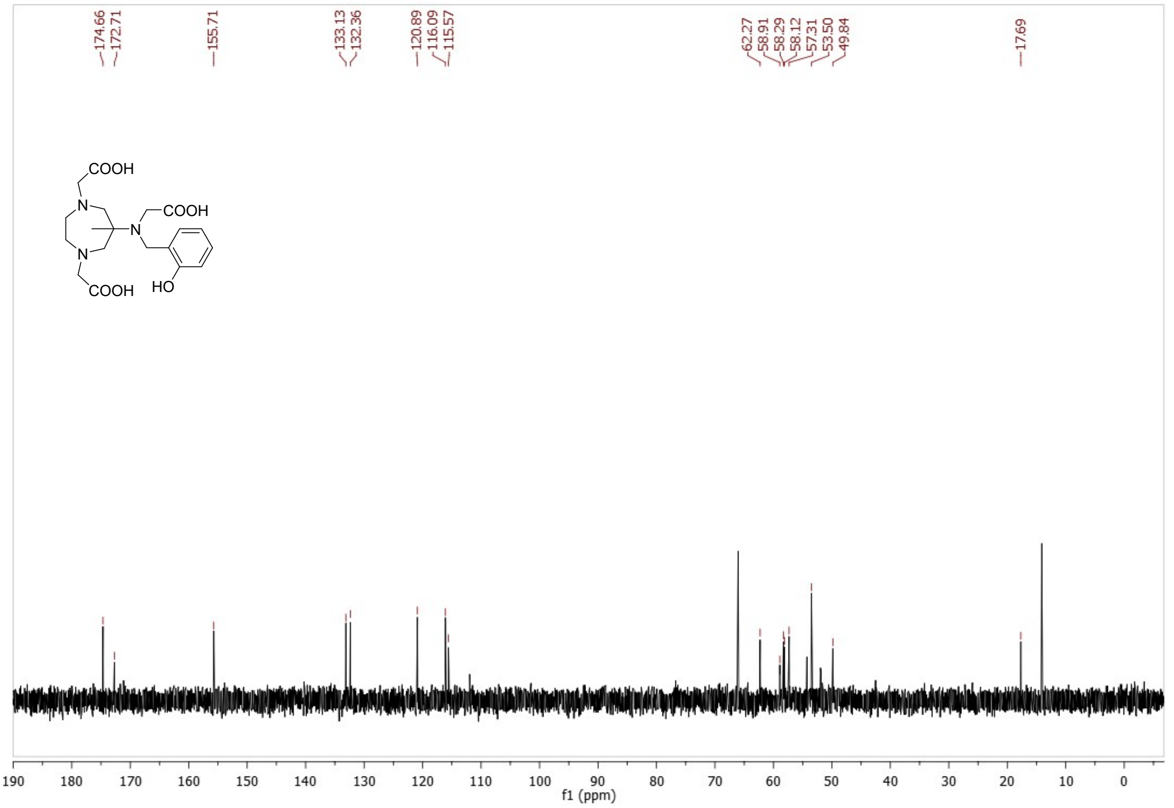

Figure S21. ^{13}C NMR spectrum in D_2O of ligand AAZ3A-exoHB (signals from residual Et_2O are also observable).

7. Bibliography

1 N. T. Beck and I. Nagypal, *Chemistry of Complex Equilibria*, Akadémia Kiadó Budapest and Nostrand Reinhold Company Ltd., London, 1990.

2 Z. Baranyai, F. Uggeri, G. B. Giovenzana, A. Benyei, E. Bruecher and S. Aime, *Chem. Eur. J.*, 2009, **15**, 1696–1705.

3 A. Vagner, E. Gianolio, S. Aime, A. Maiocchi, I. Toth, Z. Baranyai and L. Tei, *Chem. Commun.*, 2016, **52**, 11235–11238.